

# Measurements of $CP$ Violation in $B$ Meson decays at Belle

Himansu Bhusan Sahoo on behalf of the Belle Collaboration

Department of Physics and Astronomy, University of Hawaii, Honolulu, HI 96822, USA  
 himansu@phys.hawaii.edu

In this proceeding, we report the recent measurements of time-dependent  $CP$  violation in  $B$  meson decays from the Belle Collaboration. The Belle experiment stopped operation in June 2010 and collected nearly  $772 \times 10^6$   $B\bar{B}$  pairs at the  $\Upsilon(4S)$  resonance at the KEKB asymmetric-energy  $e^+e^-$  collider. We used this full data sample to measure the  $CP$  violation parameters in  $b \rightarrow c\bar{c}s$  and  $b \rightarrow c\bar{c}d$  decays. We also report new measurements of  $CPT$  violation parameters in  $B$  decays. Furthermore, we report the first observation of a new  $b \rightarrow s$  radiative penguin decay  $B^0 \rightarrow \phi K^0 \gamma$ , as well as measurements of its time-dependent  $CP$  asymmetry.

## 1. Introduction

In the standard model (SM),  $CP$  violation in  $B^0$  meson decays originates from an irreducible complex phase in the  $3 \times 3$  Cabibbo-Kobayashi-Maskawa (CKM) mixing matrix [1]. The unitarity condition of the CKM matrix gives rise to a relation  $V_{ud}V_{ub}^* + V_{cd}V_{cb}^* + V_{td}V_{tb}^* = 0$ , which can be represented by a triangle in the complex plane, known as the Unitarity Triangle (UT). The main objective of the  $B$ -factories is to test the SM picture of the origin of  $CP$  violation by measuring the angles (denoted by  $\phi_1$ ,  $\phi_2$  and  $\phi_3$ )<sup>1</sup> and sides of the UT using different  $B$  decays. In this proceeding, we report the recent measurements of time-dependent  $CP$  asymmetries in  $B \rightarrow$  Charmonium  $K^0$  decays. These proceed via  $b \rightarrow c\bar{c}s$  tree diagram and provide a precise measurement of the angle  $\phi_1$  ( $\equiv \pi - \arg(V_{tb}^*V_{td}/V_{cb}^*V_{cd})$ ). For such decays the interference between the tree amplitude and the amplitude from  $B^0 - \bar{B}^0$  mixing is dominated by the single phase  $\phi_1$ . The other modes which allows measurements of  $\phi_1$  are  $b \rightarrow c\bar{c}d$  transitions like  $B^0 \rightarrow D^+D^-$  and  $B^0 \rightarrow D^{*+}D^{*-}$ . These modes are dominated by tree diagrams, but loops may contribute. So, sensitivity to new physics (NP) increases in these decays.

On the other hand, rare radiative  $B$  meson decays are flavor changing neutral currents, forbidden at tree level in the SM but allowed through electroweak loop processes. The loop can be mediated by non-SM particles (for example, charged Higgs or SUSY particles) and therefore is sensitive to NP. The emitted photons in  $b \rightarrow s\gamma$  ( $\bar{b} \rightarrow \bar{s}\gamma$ ) decays are predominantly left-handed (right-handed) in the SM, and hence the time-dependent  $CP$  asymmetry is suppressed by the quark mass ratio ( $2m_s/m_b$ ). The expected mixing-induced  $CP$  asymmetry parameter ( $\mathcal{S}$ ) is  $\mathcal{O}(3\%)$  and the direct  $CP$  asymmetry parameter ( $\mathcal{A}$ ) is  $\sim 0.6\%$  [2]. In several extensions of the SM, both photon helicities can contribute to the decay. Therefore, any significantly larger  $CP$  asymmetry would be clear evidence for NP.

## 2. Experimental Apparatus

The Belle detector is a large-solid-angle magnetic spectrometer that consists of a silicon vertex detector (SVD), a 50-layer central drift chamber (CDC), an array of aerogel threshold Cherenkov counters (ACC), a barrel-like arrangement of time-of-flight scintillation counters (TOF), and an electromagnetic calorimeter (ECL) comprised of CsI(Tl) crystals located inside a superconducting solenoid coil that provides a 1.5 T magnetic field. An iron flux-return located outside the coil is instrumented to detect  $K_L^0$  mesons and to identify muons (KLM). The detector is described in detail elsewhere [3]. Two different inner detector configurations were used. For the first sample of  $152 \times 10^6$   $B\bar{B}$  pairs, a 2.0 cm radius beampipe and a 3-layer silicon vertex detector (SVD1) were used; for the latter samples, a 1.5 cm radius beampipe, a 4-layer silicon detector (SVD2), and a small-cell inner drift chamber were used. Belle stopped operation in June 2010 and collected more than  $710 \text{ fb}^{-1}$  of data. This corresponds to a total of  $772 \times 10^6$   $B\bar{B}$  pairs at  $\Upsilon(4S)$  resonance. Out of these nearly 80% of the data sample is reprocessed with a new tracking algorithm.

<sup>1</sup>BaBar uses an alternative notation  $\beta$ ,  $\alpha$  and  $\gamma$  corresponding to  $\phi_1$ ,  $\phi_2$  and  $\phi_3$ .

### 3. Analysis Technique

In the  $B$  meson system, the  $CP$  violating asymmetry lies in the time-dependent decay rates of the  $B^0$  and  $\bar{B}^0$  decays to a common  $CP$ -eigenstate ( $f_{CP}$ ). The asymmetry can be written as:

$$\begin{aligned} \mathcal{A}_{CP}(t) &= \frac{\Gamma[\bar{B}^0(t) \rightarrow f_{CP}] - \Gamma[B^0(t) \rightarrow f_{CP}]}{\Gamma[\bar{B}^0(t) \rightarrow f_{CP}] + \Gamma[B^0(t) \rightarrow f_{CP}]} \\ &= \mathcal{S} \sin(\Delta m_d t) + \mathcal{A} \cos(\Delta m_d t) \end{aligned}$$

where

$$\mathcal{S} = \frac{2 \operatorname{Im} \lambda}{|\lambda|^2 + 1} \quad \mathcal{A} = \frac{|\lambda|^2 - 1}{|\lambda|^2 + 1}. \quad (1)$$

Here  $\Gamma(B^0(\bar{B}^0) \rightarrow f_{CP})$  is the decay rate of a  $B^0(\bar{B}^0)$  meson decays to  $f_{CP}$  at a proper time  $t$  after the production,  $\Delta m_d$  is the mass difference between the two neutral  $B$  mass eigenstates,  $\lambda$  is a complex parameter depending on the  $B^0 - \bar{B}^0$  mixing as well as the decay amplitudes of the  $B$  meson decays to the  $CP$  eigenstate. The parameter  $\mathcal{S}$  is the measure of mixing-induced  $CP$  violation, whereas  $\mathcal{A}$  is the measure of direct  $CP$  violation<sup>2</sup>.

In the  $B$  factories, in order to measure the time-dependent  $CP$  violation parameters, we fully reconstruct one neutral  $B$  meson in its decay into a  $CP$  eigenstate. From the remaining particles in the event, the vertex of the other  $B$  meson is reconstructed and its flavor is identified. In the decay chain  $\Upsilon(4S) \rightarrow B^0 \bar{B}^0 \rightarrow f_{CP} f_{\text{tag}}$ , where one of the  $B$  mesons decays at time  $t_{CP}$  to a  $CP$  eigenstate  $f_{CP}$ , which is our signal mode, and the other decays at time  $t_{\text{tag}}$  to a final state  $f_{\text{tag}}$  that distinguishes between  $B^0$  and  $\bar{B}^0$ , the decay rate has a time dependence given by [4]

$$\mathcal{P}(\Delta t) = \frac{e^{-|\Delta t|/\tau_{B^0}}}{4\tau_{B^0}} \left\{ 1 + q \cdot \left[ \mathcal{S} \sin(\Delta m_d \Delta t) + \mathcal{A} \cos(\Delta m_d \Delta t) \right] \right\}. \quad (2)$$

Here  $\tau_{B^0}$  is the neutral  $B$  lifetime,  $\Delta t = t_{CP} - t_{\text{tag}}$ , and the  $b$ -flavor charge  $q$  equals  $+1$  ( $-1$ ) when the tagging  $B$  meson is identified as  $B^0$  ( $\bar{B}^0$ ). Since the  $B^0$  and  $\bar{B}^0$  are approximately at rest in the  $\Upsilon(4S)$  center-of-mass system,  $\Delta t$  can be determined from the displacement in  $z$  between the  $f_{CP}$  and  $f_{\text{tag}}$  decay vertices:  $\Delta t \simeq \Delta z / (\beta \gamma c)$ , where  $c$  is the speed of light. The vertex position of the  $f_{CP}$  decay is reconstructed using charged tracks (for example, lepton tracks from  $J/\psi$  in  $B^0 \rightarrow J/\psi K_S^0$  decays) and that of the  $f_{\text{tag}}$  decay from well-reconstructed tracks that are not assigned to  $f_{CP}$  [5]. The  $\Delta z$  is approximately  $200 \mu\text{m}$  in Belle and  $250 \mu\text{m}$  in BaBar. We also consider the effect of detector resolution and mis-identification of the flavor [6]. We use a flavor tagging algorithm to obtain the  $b$ -flavor charge  $q$  and a tagging quality factor  $r \in [0, 1]$ . The value  $r = 0$  signifies no flavor discrimination while  $r = 1$  implies unambiguous flavor assignment. The data are divided into seven  $r$  intervals. Finally, the  $CP$  violation parameters are obtained from an unbinned maximum likelihood (UML) fit to the  $\Delta t$  distribution.

### 4. $b \rightarrow c\bar{c}s$ Decay Modes

The  $B \rightarrow$  Charmonium  $K^0$  decays that are mediated by  $b \rightarrow c\bar{c}s$  decays are known as the golden modes for  $CP$  violation measurements. They have clean experimental signatures: many accessible modes with relatively large branching fractions  $\mathcal{O}(10^{-4})$ , low experimental background levels and high reconstruction efficiencies. These modes are dominated by a color-suppressed  $b \rightarrow c\bar{c}s$  tree diagram and the dominant penguin diagram has the same weak phase. The  $CP$  violation comes from the  $V_{td}$  element in the mixing box diagram, which contains the phase. For  $f_{CP}$  final states resulting from a  $b \rightarrow c\bar{c}s$  transition, the SM predicts  $\mathcal{S} = -\xi_{CP} \sin 2\phi_1$  and  $\mathcal{A} = 0$ , where  $\xi_{CP}$  is the  $CP$  eigenvalue of the final state and is  $+1$  ( $-1$ ) for  $CP$ -even ( $CP$ -odd) states. The asymmetry is given as

$$\mathcal{A}_{CP} = -\xi_{CP} \sin(2\phi_1) \sin(\Delta m \Delta t). \quad (3)$$

---

<sup>2</sup>Note that BaBar uses the convention  $\mathcal{C} = -\mathcal{A}$ .

We can verify this experimentally by measuring the number of  $B^0(\bar{B}^0)$  decays to  $CP$  eigenstates. A non-zero value of  $\mathcal{A}$  or any measurement of  $\sin 2\phi_1$  that has a significant deviation indicates evidence for NP.

Belle recently reported new measurements with its full data sample using the modes  $B^0 \rightarrow J/\psi K^0$ ,  $B^0 \rightarrow \psi' K_S^0$  and  $B^0 \rightarrow \chi_{c1} K_S^0$ . The  $J/\psi$  candidates are reconstructed from their decays to  $e^+e^-$  and  $\mu^+\mu^-$ , with the  $K_S^0$  reconstructed from  $\pi^+\pi^-$ . The  $\psi'$  candidates are reconstructed from  $e^+e^-$ ,  $\mu^+\mu^-$  as well as  $J/\psi\pi^+\pi^-$  decays. The  $\chi_{c1}$  is reconstructed from its decays to  $J/\psi\gamma$ .  $B$  candidates are identified using two kinematic variables: the energy difference  $\Delta E \equiv E_B^{\text{cms}} - E_{\text{beam}}^{\text{cms}}$  and the beam-energy-constrained mass  $M_{\text{bc}} \equiv \sqrt{(E_{\text{beam}}^{\text{cms}}/c^2)^2 - (p_B^{\text{cms}}/c)^2}$ , where  $E_B^{\text{cms}}$  is the beam energy in the cms, and  $E_B^{\text{cms}}$  and  $p_B^{\text{cms}}$  are the center-of-mass (cms) energy and momentum, respectively, of the reconstructed  $B$  candidate. Belle reported nearly 15600  $CP$ -odd signal events with a purity of 96% and nearly 10000  $CP$ -even signal events with a purity of 63%. Belle observed  $CP$  violation in all the listed charmonium modes and the results are summarized in Table I.

Table I: The  $CP$ -violating parameters measured by Belle with golden modes using a data sample (the errors are statistical only). Belle observed  $CP$  violation in all charmonium modes.

Decay Mode	$\mathcal{S}$	$\mathcal{A}$
$B^0 \rightarrow J/\psi K_S^0$	$0.671 \pm 0.029$	$-0.014 \pm 0.021$
$B^0 \rightarrow J/\psi K_L^0$	$-0.641 \pm 0.047$	$0.019 \pm 0.026$
$B^0 \rightarrow \psi' K_S^0$	$0.739 \pm 0.079$	$0.103 \pm 0.055$
$B^0 \rightarrow \chi_{c1} K_S^0$	$0.636 \pm 0.117$	$-0.023 \pm 0.083$

Figure 1 shows the background-subtracted  $\Delta t$  distributions and the raw asymmetry for good-tagged events only ( $r > 0.5$ ). We combine the  $CP$ -odd states,  $B^0 \rightarrow J/\psi K_S^0$ ,  $B^0 \rightarrow \psi' K_S^0$  and  $B^0 \rightarrow \chi_{c1} K_S^0$  together. We define the raw asymmetry in each  $\Delta t$  bin as  $(N_+ - N_-)/(N_+ + N_-)$ , where  $N_+$  ( $N_-$ ) is the number of observed candidates with  $q = +1$  ( $-1$ ). The systematic uncertainties are improved compared to previous Belle measurements [7, 8].

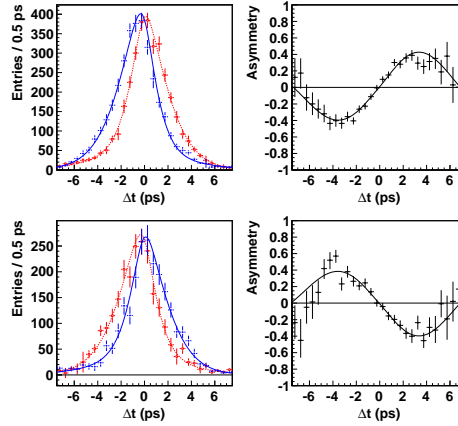


Figure 1:  $\Delta t$  distributions for  $q = +1$  (red) and  $q = -1$  (blue) and the raw asymmetry plots for  $CP$ -odd states (upper) and a  $CP$ -even ( $B^0 \rightarrow J/\psi K_L^0$ ) state (lower). These are background-subtracted and for good-tagged events only. The opposite  $CP$  asymmetry of  $B^0 \rightarrow J/\psi K_L^0$  is clearly visible from the lower plots.

Combining all charmonium modes, Belle reported the world's most precise measurements:

$$\begin{aligned} \sin 2\phi_1 &= 0.668 \pm 0.023 \pm 0.013, \\ \mathcal{A} &= 0.007 \pm 0.016 \pm 0.013, \end{aligned} \quad (4)$$

where the uncertainties are statistical and systematic, respectively.

Combining this new measurements from Belle with BaBar [9], the new world average calculated by the Heavy Flavor Averaging Group (HFAG) [10] is:

$$\begin{aligned} \sin 2\phi_1(b \rightarrow c\bar{c}s) &= 0.678 \pm 0.020, \\ \mathcal{A}(b \rightarrow c\bar{c}s) &= -0.013 \pm 0.017. \end{aligned} \quad (5)$$

The experimental uncertainty on  $\sin 2\phi_1$  is reduced to 3% and thus serves as a firm reference point for the SM. The value of  $\mathcal{A}$  is consistent with zero. The new results provide a better constraint on the allowed region in the CKM fitter as shown in Fig. 2 and give the value of  $\phi_1(\beta)$  to be [10]

$$\phi_1(\beta) = (21.4 \pm 0.8)^\circ, \quad (6)$$

which is the most precise measurement having an error  $< 1^\circ$ . Details on the measurements of the CKM angle  $\phi_1/\beta$  at the  $B$  factories are described in the FPCP 2011 proceeding [11].

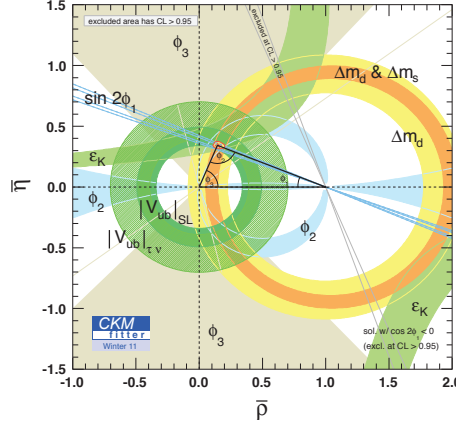


Figure 2: The global fit result from the CKM fitter using all the recent measurements of the unitary triangle.

## 5. $b \rightarrow c\bar{c}d$ Decay Modes

Belle updated the measurements of  $CP$  violation parameters in  $b \rightarrow c\bar{c}d$  decays,  $B^0 \rightarrow D^+D^-$  and  $B^0 \rightarrow D^{*+}D^{*-}$ , using the full data sample. The dominant contribution in these decays is from the tree-diagram. If this is the only contribution, then SM expectation is  $\mathcal{S} = -\sin 2\phi_1$  and  $\mathcal{A} = 0$ . But, penguin contributions are expected to change the values by a few percent [12]. Large deviations from  $\sin 2\phi_1$  in  $b \rightarrow c\bar{c}s$  decays will be clear hint of NP.

### 5.1. $B^0 \rightarrow D^+D^-$

The  $D$  mesons are reconstructed using the  $D^+ \rightarrow K^-\pi^+\pi^+$ ,  $D^+ \rightarrow K_S^0\pi^+$  and  $D^+ \rightarrow K_S^0\pi^+\pi^0$  decays [13]. Signal is extracted from an extended UML fit to the two-dimensional  $\Delta E$ - $M_{bc}$  distribution. The projections of the fit onto  $M_{bc}$  for each mode are shown in Fig. 3. Contributions from  $B^0 \rightarrow D^+K^{(*)0}\pi^-$  peaking background are estimated using a  $D$  mass sideband in data and are subtracted from the signal yield. The signal yields and measured branching fractions for each channel are summarized in the Table II.

Table II: Signal yields and measured branching fractions in each channel for the  $B^0 \rightarrow D^+D^-$  mode.

Decay Mode	Signal Yield	Branching Fraction
$(K^-\pi^+\pi^+)(K^+\pi^-\pi^-)$	$221.4 \pm 18.6$	$(2.16 \pm 0.18) \times 10^{-4}$
$(K^-\pi^+\pi^+)(K_S^0\pi^-)$	$48.0 \pm 8.9$	$(1.96 \pm 0.36) \times 10^{-4}$
$(K^-\pi^+\pi^+)(K_S^0\pi^-\pi^0)$	$54.1 \pm 14.6$	$(1.83 \pm 0.49) \times 10^{-4}$

Combining the three decay modes, we measure the branching fraction to be

$$\mathcal{B}(B^0 \rightarrow D^+D^-) = (2.09 \pm 0.15 \pm 0.18) \times 10^{-4}. \quad (7)$$

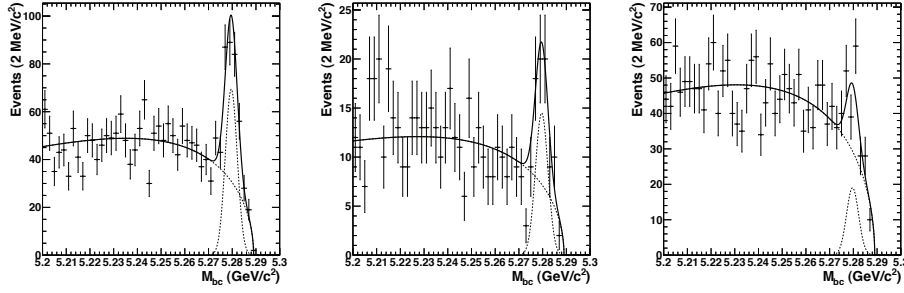


Figure 3: The  $B^0 \rightarrow D^+ D^-$   $M_{bc}$  distributions for  $K\pi\pi$  (left),  $K_S^0\pi$  (middle) and  $K_S^0\pi\pi^0$  mode (right).

This measurement is consistent with Belle's previous result using  $535 \times 10^6$   $B\bar{B}$  pairs [14]. The dominant contributions to the systematic uncertainty come from the  $K/\pi$  selection efficiency, daughter branching fractions and continuum suppression.

We use the  $K\pi\pi$  and  $K_S^0\pi$  modes in the time-dependent measurement. These modes show no significant peaking background in contrast to the  $K_S^0\pi\pi^0$  mode. The measured  $CP$  violation parameters are

$$\begin{aligned} \mathcal{S} &= -1.06 \pm 0.21(\text{stat}) \pm 0.07(\text{syst}) \text{ and} \\ \mathcal{A} &= +0.43 \pm 0.17(\text{stat}) \pm 0.04(\text{syst}). \end{aligned} \quad (8)$$

The  $\mathcal{S}$  value is consistent with the measurement from  $b \rightarrow c\bar{c}s$  decays. Compared to the previous Belle publication [14] the direct  $CP$  violation parameter ( $\mathcal{A}$ ) decreased and its central value moved towards the expected value, which is close to zero. The  $\Delta t$  distributions and raw asymmetry for  $B^0 \rightarrow D^+ D^-$  are shown in the Fig. 4.

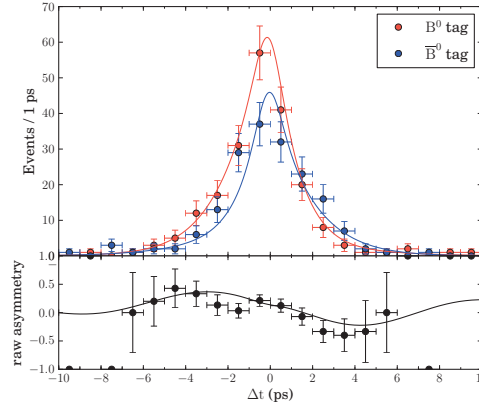


Figure 4:  $\Delta t$  distributions for  $q = +1$  (red) and  $q = -1$  (blue) (upper) and the raw asymmetry (lower) of the combined  $CP$  fit of  $k\pi\pi$  and  $K_S^0\pi$  modes in  $B^0 \rightarrow D^+ D^-$ .

## 5.2. $B^0 \rightarrow D^{*+} D^{*-}$

Belle also updated the measurements of the branching fraction, polarization and  $CP$  violation parameters for  $B^0 \rightarrow D^{*+} D^{*-}$  using the full data sample. The signal is reconstructed in a total of nine hadronic  $D$  decay modes. The signal yield is obtained from a two-dimensional extended UML fit to the  $\Delta E - M_{bc}$  distribution. We obtain a signal yield of  $1225 \pm 59$  events and the measured branching fraction is

$$\mathcal{B}(B^0 \rightarrow D^{*+} D^{*-}) = (7.82 \pm 0.38 \pm 0.60) \times 10^{-4}. \quad (9)$$

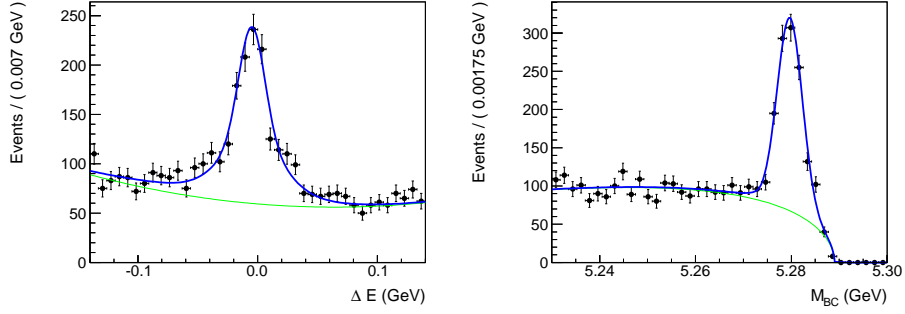


Figure 5:  $\Delta E$  (left) and  $M_{bc}$  (right) distributions for  $B^0 \rightarrow D^{*+}D^{*-}$  mode.

We have a large gain in signal yield compared to Belle's previous publication with  $657 \times 10^6 B\bar{B}$  pairs [15] due to higher track multiplicity in the final state.

$B^0 \rightarrow D^{*+}D^{*-}$  is the decay of a scalar to two vector mesons; the final state is a mixture of  $CP$ -even and  $CP$ -odd states. Therefore, an angular analysis has to be performed to determine the fraction of  $CP$ -even decays. This is done using two of the three possible angles of the transversity base, denoted by  $\cos\theta_{tr}$  and  $\cos\theta_1$ . The measurements of polarization and  $CP$  violation are performed simultaneously with a five dimensional fit to  $\Delta E$ ,  $M_{bc}$ ,  $\cos\theta_{tr}$ ,  $\cos\theta_1$  and  $\Delta t$  distributions. The  $\cos\theta_{tr}$  and  $\cos\theta_1$  distributions for data in the signal region of  $\Delta E$ - $M_{bc}$  are shown in Fig. 6.

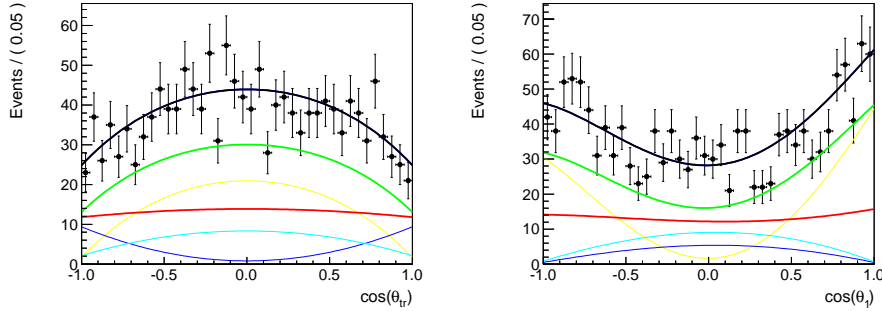


Figure 6: The projections of the angular distributions in the signal region of  $\Delta E$  and  $M_{bc}$ . The black (green, red) line shows the total (signal, background) pdf, while orange, blue and cyan lines show the signal contributions for each of the polarization states.

We measure the polarization and  $CP$  violation parameters to be

$$\begin{aligned}
 \mathcal{S} &= -0.79 \pm 0.13 \pm 0.03 \\
 \mathcal{A} &= +0.15 \pm 0.08 \pm 0.02 \\
 \mathcal{R}_0 &= 0.62 \pm 0.03 \pm 0.01 \\
 \mathcal{R}_\perp &= 0.14 \pm 0.02 \pm 0.01
 \end{aligned}
 \tag{10}$$

Both the measurements of branching fraction and the polarization are consistent with Belle's previous measurement [15]. The  $CP$  violation parameters are consistent with SM predictions.

The HFAG summary of the  $b \rightarrow c\bar{c}d$  results from Belle and BaBar are shown in Fig. 8.

## 6. CPT violation parameters in $B^0$ decay

$CPT$  conservation is one of the most fundamental laws in the SM. Any evidence of  $CPT$  violation will be clear hint of NP. Using a data sample of  $535 \times 10^6 B\bar{B}$  pairs, we measure the  $CPT$  violating parameter in  $B^0 \rightarrow J/\psi K_S^0$ ,  $B^0 \rightarrow J/\psi K_L^0$ ,  $B^0 \rightarrow D^-\pi^+$ ,  $B^0 \rightarrow D^{*-}\pi^+$ ,  $B^0 \rightarrow D^{*-}\rho^+$  and  $B^0 \rightarrow D^{*-}l^+\nu_l$  decays.

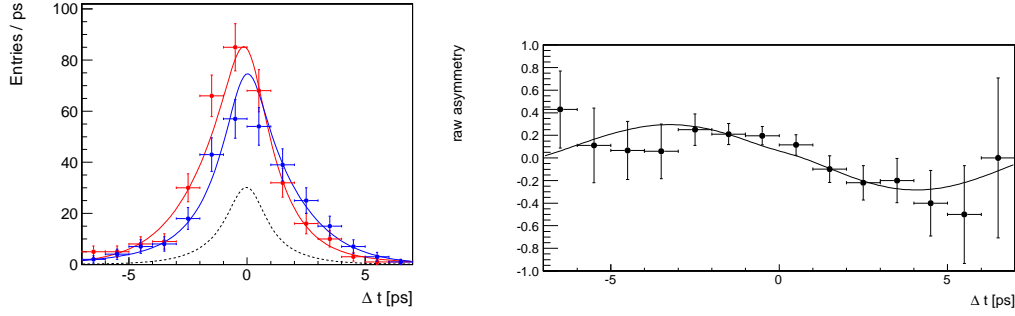


Figure 7:  $\Delta t$  distributions for  $q = +1$  (red) and  $q = -1$  (blue) (left) and the raw asymmetry plot (right) for  $B^0 \rightarrow D^{*+} D^{*-}$  mode. These are for good-tagged events only.

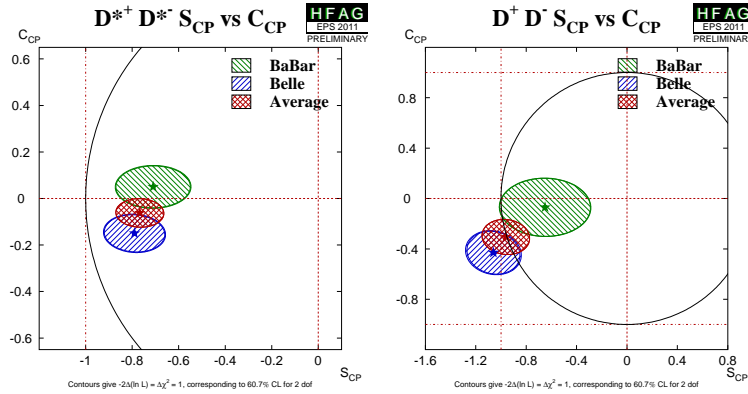


Figure 8: The HFAG summary of the results on  $B^0 \rightarrow D^+ D^-$  and  $B^0 \rightarrow D^{*+} D^{*-}$  from  $B$  factories.

Assuming  $CPT$  violation, we can express the mass eigenstates of the  $B$  meson as a linear combination of weak eigenstates by introducing a complex number  $z$  in  $B^0$ - $\bar{B}^0$  mixing. Any non-zero value of  $z$  (in either the real or the imaginary term) will indicate  $CPT$  violation in mixing. The decay modes  $B^0 \rightarrow J/\psi K_S^0$  and  $B^0 \rightarrow J/\psi K_L^0$  are sensitive to  $\text{Re}(z)$  and  $\Delta\Gamma_d/\Gamma_d$ , while the modes  $B^0 \rightarrow D^- \pi^+$ ,  $B^0 \rightarrow D^{*-} \pi^+$ ,  $B^0 \rightarrow D^{*-} \rho^+$  and  $B^0 \rightarrow D^{*-} l^+ \nu_l$  are sensitive to  $\text{Im}(z)$ . The charged modes  $B^+ \rightarrow J/\psi K^+$  and  $B^+ \rightarrow D^0 \pi^+$  are used to determine the  $\Delta t$  resolution. We have a total of 534,068 neutral  $B$  and 248,775 charged  $B$  events.

Using an UML fit to 72 free parameters, we measure the  $CPT$  violating parameters as

$$\begin{aligned} \text{Re}(z) &= (+1.9 \pm 3.7 \pm 3.2) \times 10^{-2}, \\ \text{Im}(z) &= (-5.7 \pm 3.3 \pm 6.0) \times 10^{-2}, \\ \Delta\Gamma_d/\Gamma_d &= (-1.7 \pm 1.8 \pm 1.1) \times 10^{-2}. \end{aligned} \quad (11)$$

The results are consistent with zero. The  $\Delta t$  distribution for  $B^0 \rightarrow J/\psi K_S^0$  is shown in Fig. 9.

## 7. First Observation of $B^0 \rightarrow \phi K_S^0 \gamma$ decay

Using the full data sample we observed for the first time the neutral mode  $B^0 \rightarrow \phi K_S^0 \gamma$  [17]. We measure the branching fractions for both charged  $B^+ \rightarrow \phi K^+ \gamma$  and neutral  $B^0 \rightarrow \phi K^0 \gamma$ , with  $\phi \rightarrow K^+ K^-$  and  $K_S^0 \rightarrow \pi^+ \pi^-$ . The signal yield is obtained from an extended UML fit to the two-dimensional  $\Delta E$ - $M_{bc}$  distribution. The dominant background comes from  $e^+ e^- \rightarrow q\bar{q}$  ( $q = u, d, s, c$ ) continuum events. Another significant background is non-resonant (NR)  $B \rightarrow K^+ K^- K \gamma$ , which peaks in the  $\Delta E$ - $M_{bc}$  signal region; it is estimated using the  $\phi$  mass sideband,  $M_{K^+ K^-} \in [1.05, 1.30]$  GeV/ $c^2$ , in data. The projections of the fit results onto  $M_{bc}$  are shown

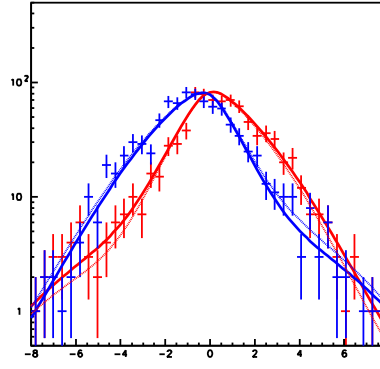


Figure 9:  $\Delta t$  distributions for  $q = +1$  (red) and  $q = -1$  (blue) for  $B^0 \rightarrow J/\psi K_S^0$  mode with good flavor tag events only. The light lines indicate  $\mathcal{R}e(z) = 0.2$  and  $\mathcal{I}m(z) = 0.0$ .

in Fig. 10. The fit yields a signal of  $144 \pm 17$   $B^+ \rightarrow \phi K^+ \gamma$  and  $37 \pm 8$   $B^0 \rightarrow \phi K_S^0 \gamma$  candidates. The signals in the charged and neutral modes have significances of  $9.6\sigma$  and  $5.4\sigma$ , respectively.

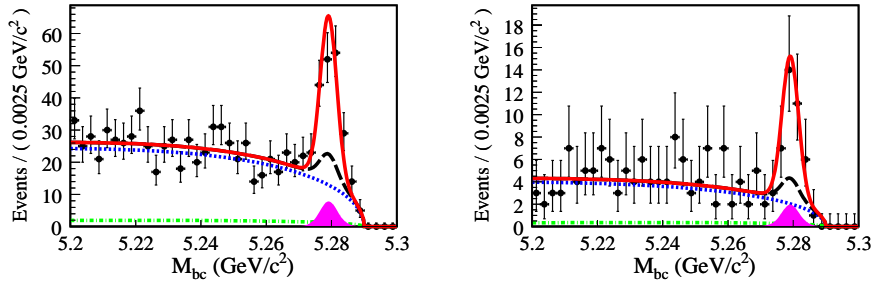


Figure 10:  $M_{bc}$  projections for  $B^+ \rightarrow \phi K^+ \gamma$  (left) and  $B^0 \rightarrow \phi K_S^0 \gamma$  (right). The points with error bars are the data. The curves show the total fit function (solid red), total background function (long-dashed black), continuum component (dotted blue), the  $b \rightarrow c$  component (dashed-dotted green) and the non-resonant component as well as other charmless backgrounds (filled magenta histogram).

To measure the  $M_{\phi K}$  distribution, we repeat the fit in bins of  $\phi K$  mass and the resulting signal yields are corrected for the detection efficiency. Nearly 72% of the signal events are concentrated in the low-mass region,  $M_{\phi K} \in [1.5, 2.0]$   $\text{GeV}/c^2$ . The background-subtracted and efficiency-corrected  $M_{\phi K}$  distributions are shown in Fig. 11. These spectra are consistent with the expectations from the pQCD model for non-resonant  $B \rightarrow \phi K \gamma$  decays [16]. The form factor effect produces the peak at the threshold. With the present statistics no clear evidence is found for the existence of a kaonic resonance decaying to  $\phi K$ . The reconstruction efficiencies after reweighting according to this  $M_{\phi K}$  dependence are  $(15.3 \pm 0.1(\text{stat}))\%$  for the charged mode and  $(10.0 \pm 0.1(\text{stat}))\%$  for the neutral mode. The measured branching fractions are [17]

$$\begin{aligned} \mathcal{B}(B^+ \rightarrow \phi K^+ \gamma) &= (2.48 \pm 0.30 \pm 0.24) \times 10^{-6} \text{ and} \\ \mathcal{B}(B^0 \rightarrow \phi K^0 \gamma) &= (2.74 \pm 0.60 \pm 0.32) \times 10^{-6}. \end{aligned} \quad (12)$$

We also measure the charge asymmetry in  $B^\pm \rightarrow \phi K^\pm \gamma$  decay to be [17]

$$\mathcal{A}_{CP} = [N(B^-) - N(B^+)]/[N(B^-) + N(B^+)] = -0.03 \pm 0.11 \pm 0.08, \quad (13)$$

where  $N(B^-)$  and  $N(B^+)$  are the signal yields for  $B^-$  and  $B^+$  decays, respectively.

We also performed the first time-dependent measurements in the neutral  $B^0 \rightarrow \phi K_S^0 \gamma$  mode. In contrast to  $B^0 \rightarrow K^{*0}(\rightarrow K_S^0 \pi^0) \gamma$ , another related mode that is sensitive to NP, the time dependence of  $B^0 \rightarrow \phi K_S^0 \gamma$  can be measured from the  $\phi \rightarrow K^+ K^-$  decay and does not require a difficult measurement of the long lived  $K_S^0$  decay inside the inner tracking volume or reconstruction of a low energy  $\pi^0$ . The vertex position of the signal



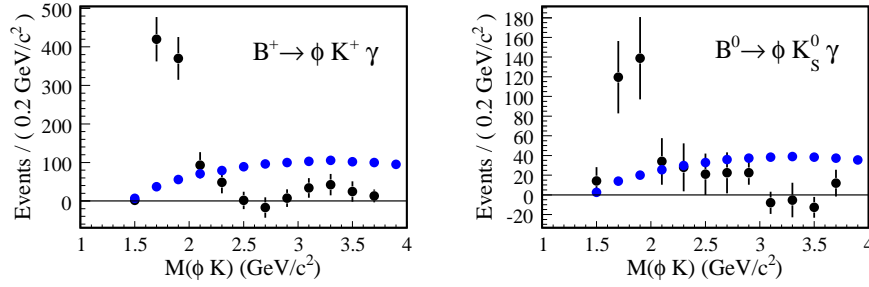


Figure 11: Background-subtracted and efficiency-corrected  $\phi K$  mass distributions for the charged (left) and neutral (right) modes. The points with error bars represent the data. The yield in each bin is obtained by the fitting procedure described in the text. A three-body phase-space model from MC simulation is shown by the filled circles (blue points) and normalized to the total data signal yield.

side is reconstructed using the two kaon tracks from the  $\phi$  meson. Since the NR component is expected to have the same NP as the signal  $B \rightarrow \phi K \gamma$ , we treat this as signal for the time-dependent fit.

The measured  $CP$  violation parameters are [17]

$$\begin{aligned} \mathcal{S} &= +0.74^{+0.72}_{-1.05}(\text{stat})^{+0.10}_{-0.24}(\text{syst}) \text{ and} \\ \mathcal{A} &= +0.35 \pm 0.58(\text{stat})^{+0.23}_{-0.10}(\text{syst}). \end{aligned} \quad (14)$$

We have established that the mode  $B^0 \rightarrow \phi K_S^0 \gamma$  can be used at future high luminosity  $e^+e^-$  and hadronic facilities to perform time-dependent  $CP$  violation measurements and to carry out sensitive tests for NP. The results are accepted for publication in Physical Review D [17].

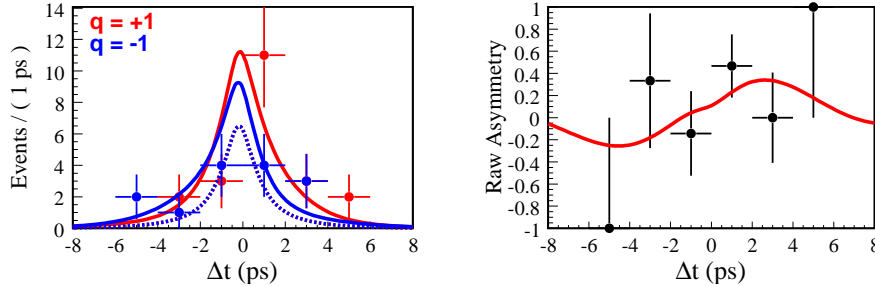


Figure 12:  $\Delta t$  distributions for  $q = +1$  and  $q = -1$  (left) and the raw asymmetry (right) for well-tagged events. The dashed curves in the  $\Delta t$  plot are the sum of backgrounds while the solid curves are the sum of signal and backgrounds. The solid curve in the asymmetry plot shows the result of the UML fit.

The HFAG summary of the results in  $b \rightarrow s \gamma$  modes from Belle and BaBar is shown in Fig. 13. With the present statistics, these measurements are consistent with the SM predictions and there is no indication of NP from right-handed currents in radiative  $B$  decays.

## 8. Summary

In summary, we have presented the recent measurements on  $CP$  violation parameters from Belle using the full data sample  $772 \times 10^6 B\bar{B}$  collected at the  $\Upsilon(4S)$  resonance. The  $CP$  violation parameters in  $b \rightarrow c\bar{c}s$  decays are the most precise measurement and provide a reference point for new physics searches. We have updated the branching fraction and  $CP$  violation results in  $B^0 \rightarrow D^+D^-$  and  $B^0 \rightarrow D^{*+}D^{*-}$  using the full data sample. These are consistent with the measurements of  $\sin 2\phi_1$  from  $b \rightarrow c\bar{c}s$  decays. We also presented the first measurements of  $CPT$  violation parameters in  $B$  decays, which are consistent with zero. The first observation of  $B^0 \rightarrow \phi K^0 \gamma$  and its  $CP$  violation parameters are also reported. This mode establishes a new method for searching right-handed currents and will be used in future very high luminosity experiments.

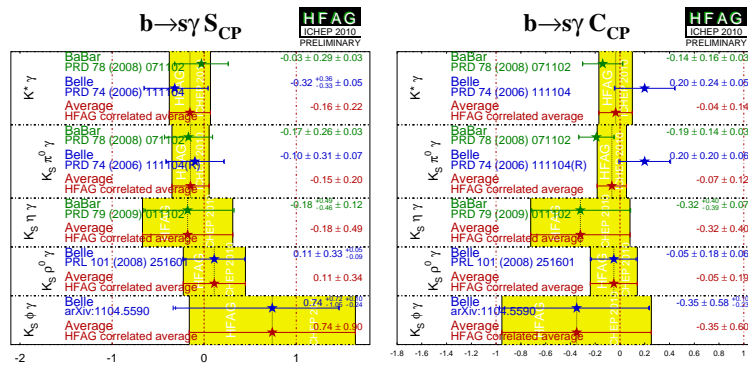


Figure 13: The HFAG summary of the TCPV results in exclusive  $b \rightarrow s\gamma$  decays from  $B$  factories.

## Acknowledgments

I would like to thank my Belle colleagues for giving me opportunity to present the recent results on  $CP$  violation measurements. We thank the KEKB group for excellent operation of the accelerator, the KEK cryogenics group for efficient solenoid operations, and the KEK computer group and the NII for valuable computing and SINET3 network support. We acknowledge support from MEXT, JSPS and Nagoya's TLPRC (Japan); ARC and DIISR (Australia); NSFC (China); MSMT (Czechia); DST (India); MEST, NRF, NSDC of KISTI, and WCU (Korea); MNiSW (Poland); MES and RFAAE (Russia); ARRS (Slovenia); SNSF (Switzerland); NSC and MOE (Taiwan); and DOE (USA).

## References

- 1 N. Cabibbo, Phys. Rev. Lett. **10**, 531 (1963); M. Kobayashi and T. Maskawa, Prog. Theor. Phys. **49**, 652 (1973).
- 2 D. Atwood, M. Gronau and A. Soni, Phys. Rev. Lett. **79**, 185 (1997). D. Atwood, T. Gershon, M. Hazumi and A. Soni, Phys. Rev. D **71**,
- 3 A. Abashian *et al.* (Belle Collaboration), Nucl. Instrum. Methods Phys. Res., Sect. A **479**, 117 (2002).
- 4 A. B. Carter and A. I. Sanda, Phys. Rev. D **23**, 1567 (1981); I. I. Bigi and A. I. Sanda, Nucl. Phys. B **193**, 85 (1981).
- 5 H. Tajima *et al.*, Nucl. Instrum. Methods Phys. Res., Sect. A **533**, 370 (2004).
- 6 H. Kakuno *et al.*, Nucl. Instrum. Methods Phys. Res., Sect. A **533**, 516 (2004).
- 7 K.-F. Chen *et al.* (Belle Collaboration), Phys. Rev. Lett. **98**, 031802 (2007).
- 8 H. Sahoo *et al.* (Belle Collaboration), Phys. Rev. D **77**, 091103 (2008).
- 9 B. Aubert *et al.* (BaBar Collaboration), Phys. Rev. D **79**, 072009 (2009).
- 10 Heavy Flavor Averaging Group, winter 2011 update. Check their webpage for updated results: <http://www.slac.stanford.edu/xorg/hfag/>.
- 11 H. Sahoo, for the Belle and BaBar Collaborations, arXiv:1107.0503 [hep-ex], published in the proceedings of FPCP 2011, Maale Hachamisha, Israel, May 23-27, 2011.
- 12 Z.-Z. Xing, Phys. Rev. D **61**, 014010 (1999).
- 13 Throughout this proceeding, the inclusion of the charge-conjugate decay mode is implied unless otherwise stated.
- 14 S. Fratina *et al.* (Belle Collaboration), Phys. Rev. Lett **98**, 221802 (2007).
- 15 K. Vervink *et al.* (Belle Collaboration), Phys. Rev. D **80**, 111104 (2009).
- 16 C. H. Chen and H.-n. Li, Phys. Rev. D **70**, 054006 (2004) and private communication with H.-n. Li. The pQCD model is in qualitative agreement with our data after including the kinematic effect of the kaon mass.
- 17 H. Sahoo *et al.* (Belle Collaboration), arXiv:1104.5590, To be published in Physical Review D.